Nonlinear Processes in Geophysics (1994) 1: 136 - 144

Nonlinear Processes in Geophysics

Developing diagnostics for input-output systems: the effects of certain linear and nonlinear filters on the correlation integral

D. Vassiliadis[1] and I.A. Daglis[2]

[1] Laboratory for Extraterrestrial Physics, Code 692, NASA/GSFC, Greenbelt, MD 20771, USA
[2] Max-Planck-Institut für Aeronomie, 37189 Katlenburg-Lindau, Germany

Received 2 December 1993 - Accepted 13 March 1994 - Communicated by S. Lovejoy

Abstract. Input-output systems are characterized by applying time series analysis techniques developed for autonomous systems to the input and the output time series separately and using the results as nonlinear statistics of the time series distributions. Two examples are presented using the correlation integral as a nonlinear statistic: the first one examines the change in the statistic when several sample input time series are passed through a nonlinear filter. The rectifier is chosen as the filter because it models, at first approximation, the effect of dayside magnetospheric reconnection to the interplanetary magnetic field and solar wind input. The changes in the correlation integral are used to characterize the filter response. A second example compares a linear filter of the rectified solar wind input to the observed auroral geomagnetic activity in terms of their correlation integrals. Implications for models of the solar wind-magnetosphere coupling are discussed.

1 Introduction

Input-output dynamical systems are systems where one or more input signals are measured simultaneously with the system's output. The input is a nontrivial, usually irregular, function of time. Studies of stability and prediction of such systems (Hunter and Theiler, 1992; Casdagli, 1992) have extended the notions of dynamical state and Lyapunov exponent originally developed for autonomous systems. Specific applications have been made in experimental and observational environments (Hunter, 1992; Hunter and Theiler, 1992; Vassiliadis et al., 1992; Price and Prichard, 1993; Vassiliadis et al., 1994).

A *linear* input-output system is characterized and identified by the power and phase spectra of the input and output time series. In the frequency domain the ratio of output to input power spectrum gives the transfer function of the system (Rugh, 1993). In the time domain the Fourier transform of the transfer function is the impulse response which gives a "black-box" description of the linear system.

For *nonlinear* systems the characterization with spectral techniques is not possible. In the case of *autonomous* systems (where the "input" is zero, constant or periodic) several techniques have been developed to obtain *invariants*: the spectra of dimensions, entropies and Lyapunov exponents (Abarbanel et al., 1993). These techniques are used to characterize and identify system properties in ways analogous to the spectral approach for linear systems (Table 1 in (Abarbanel et al., 1993)).

In order to characterize a nonlinear input-output system, autonomous system analysis techniques are applied to the input and output time series separately. The results of the analysis ("dimensions", "entropies", etc.) are considered as nonlinear statistics that characterize the probability distribution of the time series. The changes in the statistics between input and output characterize the input-output system or "filter". Secondly the nonlinear statistics can be used to discriminate between several outputs of different models which are driven by the same input. The statistics can be used as measures of similarity between the model outputs and observations. Both applications are related to the approach of Theiler et al. (1992a,b) who used nonlinear statistics to quantify the similarity of model-derived ("surrogate") data with observations and thus establish a hypothesis testing methodology to detect nonlinear structure in time series.

In the following sections two nonlinear statistics, the correlation integral and its local slope are computed for the input and output time series of a model nonlinear system, the rectifier. The rectifier sets the negative part of the input time series to zero while leaving the positive

Correspondence to: D. Vassiliadis

part intact. The two statistics are in general changed under the action of the rectifier in characteristic ways which are accounted for by an analytical modeling of the rectifier's effect on a class of stochastic signals.

In magnetospheric physics a rectifier is a simple way to model the dominant process in the coupling of the solar wind input to the terrestrial magnetosphere. When the interplanetary magnetic field (IMF) encounters the terrestrial field on the dayside of the magnetosphere, their field lines open and reconnect (merge) to lines of the opposite field (Dungey, 1961). The bulk of solar wind energy that is transferred to the magnetosphere enters it through merged field lines (Russell, 1986). The reconnection rate is highest when the time-dependent IMF field is antiparallel to the fixed (Northward at the equator) direction of the terrestrial field. At first approximation the reconnection acts as a rectifier, being on when the B_z component of the IMF points Southward and turning off when it is parallel to the magnetospheric field. Theenergy input rate to the magnetosphere is proportional to the solar wind's convection electric field vB_z passed through a negative rectifier:

$$vB_{South} \equiv \begin{cases} -vB_z, & B_z < 0 \\ 0, & B_z \geq 0 \end{cases} \quad (1)$$

The flow speed v gives the convection rate of IMF and its changes are much slower than the autocorrelation time for the rectified IMF B_z component (1–3 h).

The solar wind and IMF energy that enters the magnetosphere during reconnection is stored in the magnetosphere. Geomagnetic storm and substorm activity depends on the rectified solar wind electric field as well as the stored earlier input (McPherron, 1991). The magnetospheric dynamics acts as a further nonlinear filter on the rectified input and produces geomagnetic activity as its output. The dynamical relation between the solar wind input and geomagnetic activity has been examined using linear (e.g. Bargatze et al., 1985), nonlinear autonomous (e.g., Baker et al., 1990; Roberts, 1991; Pavlos et al., 1992; Prichard and Price, 1992) and nonlinear input-output (Goertz et al., 1993; Price et al., 1993; Klimas et al., 1994; Vassiliadis et al., 1994) techniques. Using a discriminating nonlinear statistic one can determine the appropriateness of a class of input-output systems in modeling the coupling between solar wind and geomagnetic activity. Therefore comparative examination of the statistical properties of solar wind input and geomagnetic output have been important in solar wind-magnetosphere coupling studies.

2 The correlation integral

The correlation integral was introduced in the calculation of the correlation dimension D_2 of a time series (Grassberger and Procaccia, 1983a). After the time series data are embedded in an m-dimensional space as vectors $\mathbf{X}$ using the time-delay technique (Grassberger and Procaccia, 1983a), the correlation integral is defined as the double sum

$$C(r;m,N) = \frac{2}{N^2} \sum_{i=1}^{N} \sum_{j=i+1}^{N} \Theta(r - |\mathbf{X}_i - \mathbf{X}_j|_m) \quad (2)$$

and measures the distribution of distances r between pairs of embedding vectors $\mathbf{X}$. The time delay is set to $\tau = T_{AC}$, the autocorrelation time of the input time series. (The correction for effects of autocorrelation (Theiler, 1986) removes the fractal scaling of $1/f^{\alpha}$ noise and does not affect results significantly for the deterministic time series considered below so it will not be used here). If the integral scales exponentially

$$C \sim r^{D_2} \quad (3)$$

with the phase space distance, r, the exponent D_2 is the correlation dimension for that distribution. For deterministic autonomous systems the dimension is related to the system's degrees of freedom. For a class of stochastic systems (Gaussian linearly correlated $1/f^{\alpha}$ noise) the dimension is related to the fractal structure of the trajectory in the embedding space (Osborne and Provenzale, 1989) when the length of the time series points is low (Theiler, 1991). Here, instead of the definition of D_2, the local slope of log(C) with log(r) will be considered as a second statistic in addition to the correlation integral.

Apart from the correlation dimension several quantities are calculated from the correlation integral. If the time series come from a deterministic autonomous system, these quantities are related to the system stability (K_2 entropy (Grassberger and Procaccia, 1983b)), the complexity of its dynamics (the dimension as well as the BDS statistic (Brock, 1988)), etc. For an arbitrary time series they are used as scalar nonlinear statistics. It is still preferable to use the correlation integral than the derived statistics, since it contains more information than each one of these statistics and it has a simple interpretation because it is related to the average relative distribution of points in the embedding space.

3 Description of the time series data

The effect of the rectifier on the correlation integral is examined using several input time series separately. The first input, R(t), of 5000 points has a power spectrum decreasing roughly as $1/f^{1.6}$, its distribution is roughly Gaussian and its Fourier phases are random. For this random signal the average is negative and comparable to the standard deviation (–76:143). The negative part of the time series (R(t)<0) carries most of the power and this asymmetry gives different results for a "positive rectifier" (taking the positive part) and a "negative" one (taking the negative part). Both cases are shown to examine the effect of the bias.

The second type of input, L(t), is a deterministic signal namely the x coordinate of the Lorenz flow (Lorenz, 1963). The parameters σ=10, ρ=28, and β=8/3 result in a widely studied chaotic regime. The L(t) time series is symmetric with respect to zero and the rectifier is used to extract the positive part. Its length is also 5000 points.

Finally the analysis is applied to space physical time series. For the nonlinear solar wind- magnetosphere coupling these time series are the solar wind electric field vB_z, the rectified field vB_{South} and the simultaneous auroral geomagnetic activity index, AL. Each time series contains the first 5000 points from the data base compiled by Clauer et al. (1983).

4 Using the correlation integral to characterize an input-output system

4.1 Autocorrelation functions

The random signal R(t) has an autocorrelation time of 40 time units (solid line in Fig. 1), which decreases when taking the absolute value |R(t)| drops faster (dot–dashed line). The positive part of R(t) (dashed line), has an intermediate behavior: initially its autocorrelation coincides with that of |R(t)| while for time scales longer than the autocorrelation scale it switches over to the autocorrelation of the unrectified signal. The negative part of R(t) (dotted line) carries most of the signal power and the negative rectifier leaves it unchanged so that its autocorrelation is very similar to that of the original signal.

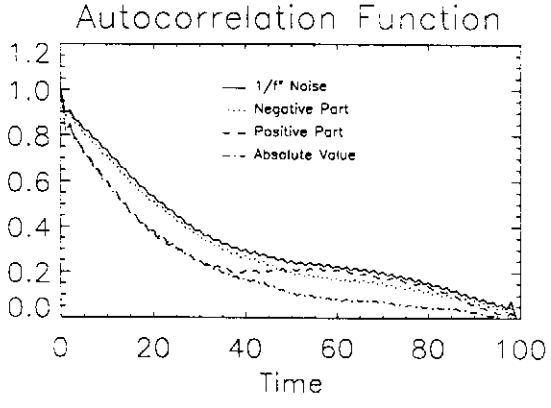

Fig. 1. The autocorrelation time of the random signal R(t) time series, of its positive and negative parts, and its absolute value.

The corresponding autocorrelation functions for L(t) are shown in Fig. 2. There is a small quantitative difference between the positive and the negative parts and they are both quite different from the autocorrelation of L(t).

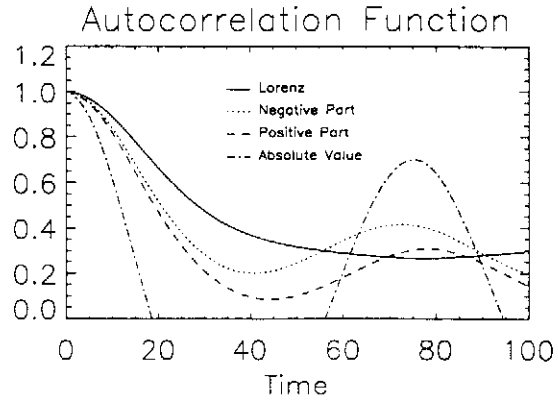

Fig. 2. The autocorrelation time of the deterministic signal L(t), of its positive and negative parts, and its absolute value.

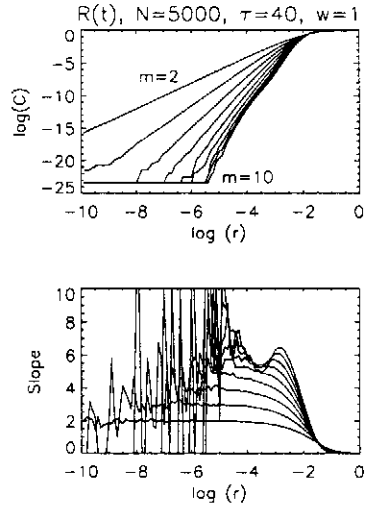

Fig. 3. The correlation integral and slope for the random signal R(t).

4.2 Correlation integrals

The correlation integral logC(logr) graph for R(t) shows a saturation at high embedding dimension m (Fig. 3). The local slope of the correlation integral (lower panel) has a maximum around 6. The fractal scaling of a stochastic $1/f^{\alpha}$ spectrum time series observed by Osborne and Provenzale (1991) and explained by Theiler (1991). The correlation integral of |R(t)| does not change significantly (Fig. 4). It increases more uniformly and shows a higher correlation dimension (>7) at m=10.

The positive part, R(t)>0, has a very different correlation integral profile (Fig. 5). There are two distinct regimes, both of which have a lower local slope than the original time series. The first regime appears at low m=2-6, while the other one is at high m=7-10. Because the embedding coordinates are lagged versions of the time series the first regime corresponds to short time scales, (m–1)τ = 40-200 units, while the second one

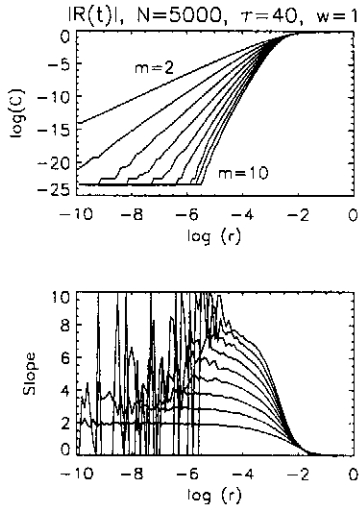

Fig. 4. Same as Fig. 3 for the absolute value |R(t)|.

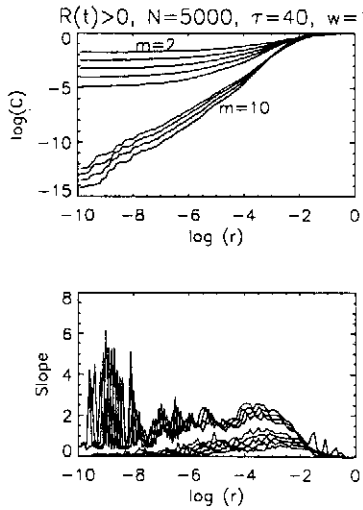

Fig. 5. Same as Fig. 3 for the positive part, R(t)>0.

to long scales, 240-360 units. Choosing a lower delay τ further decreases the slope of logC(logr).

The negative part, R(t)<0, shows an intermediate effect between Figs. 3 and 5. Because the negative part carries a much larger part of the signal power than the positive part (4:1), the local slope decreases (Fig. 6), but not as strongly as in the positive part. In addition there is no transition between two different regimes. The maximum slope is slightly lower (5.5), but there is a qualitative difference from the logC(logr) diagram of the original R(t) in that the slope increases smoothly with r and m, due to the presence of zeros in the time series which contribute to the low-r region even at high embedding dimensions.

The second time series (Lorenz flow) has a dimension of 2.1 (Fig. 7) which strongly decreases when its

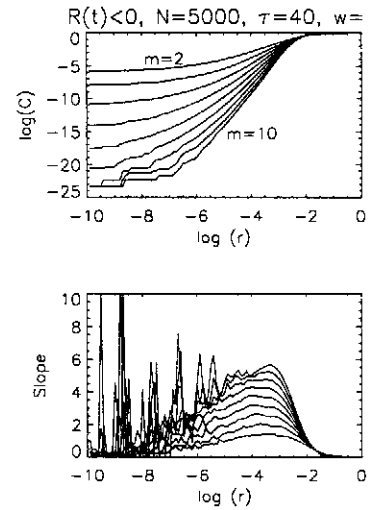

Fig. 6. Same as Fig. 3 for the negative part, R(t)<0.

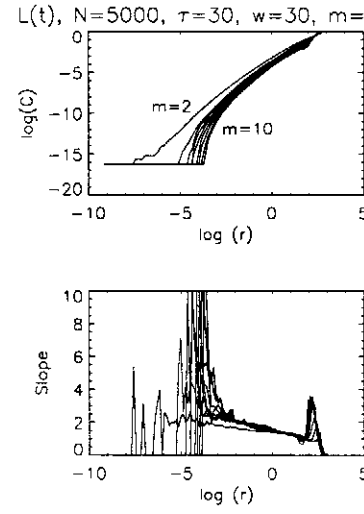

Fig. 7. The correlation integral and slope for the deterministic signal L(t).

positive part is taken (Fig. 8). The original correlation integral is not recovered for m<10. A similar effect is observed for the negative part.

4.3 The effect of the rectifier

The rectifier acts on the input signal u producing an output x

$$x = \begin{cases} u, & u > 0 \\ 0, & u \leq 0 \end{cases} \tag{4}$$

and decreases the autocorrelation of the input signal (Figs. 1–2). Embedding the input time series gives a set of vectors U=(u(n), u(n-τ), u(n-2τ), ..., u(n-(m-1)τ)) which are mapped by the rectifier to a set of vectors

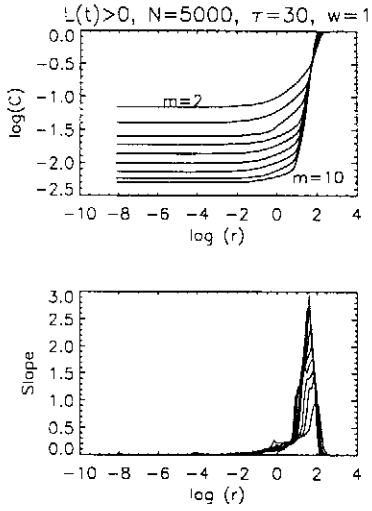

Fig. 8. Same as Fig. 7 for the positive part of the deterministic signal L(t).

constructed from x, $\mathbf{X}$=(x(n), x(n-τ), x(n-2τ), ..., x(n-(m-1)τ)).

Consider a set of successive negative points in the input u which are all mapped to x=0 by the rectifier. For m=1, the corresponding vectors $\mathbf{X}$ are also mapped to the origin of the embedding space. They are nearest neighbors with all vectors mapped to zero from negative inputs. If the positive and negative parts of u are assumed to occur equally frequently and there are very few zeroes in u, the probability density function ρ(x) is

$$\rho(x) = \frac{1}{2}\delta(x) + P(x = u > 0) \tag{5}$$

This is also the distribution of vectors $\mathbf{X}$ in the m=1-dimensional embedding space. Their number is designated by N_0 which for m=1

$$N_0 \simeq \frac{N}{2}, \qquad m = 1. \tag{6}$$

There is a high contribution to C(r) at all spatial scales r which makes the correlation integral profile with r flatter than for the input signal, u.

As m is increased, additional coordinates are attached to $\mathbf{X}$ and the number of $\mathbf{X}$=$\mathbf{0}$, N_0, decreases until there are almost no points left at the origin. At that embedding dimension the correlation integral scales similarly for the original and the rectified signals (there are still differences between the original vectors $\mathbf{U}$ and the rectified vectors $\mathbf{X}$, but the scaling of C(r) is not observed to be affected significantly). Depending on the relative length of the embedding vector's window in time (m-1)τ versus the average length of the string of zeros due to the rectifier, there is a transition from the low correlation integral to recovering the correlation integral of the input signal. If the window (m-1)τ is small (large) compared to the average length of zeros in the x time series the transition is smooth (sharp) as shown in Figs. 6, 8 (Fig. 5). The transition from the correlation integrals for the input in Figs. 3 and 7 to those of the output in Figs. 5, 6, and 8 characterize the rectifier.

4.4 Modeling the effect of the rectifier on the correlation integral of a $1/f^{\alpha}$ noise

The action of the rectifier on C(r) is calculated analytically for a Gaussian $1/f^{\alpha}$ linearly correlated noise. This is an input time series u(t) with a power spectrum $1/f^{\alpha}$ (constant below a frequency f_0 to avoid an infrared catastrophe) where $1 < \alpha < 3$, Gaussian probability distribution, and random phases. For that type of signal and using the maximum norm, Theiler (1991) calculates the correlation integral

$$C_I(r; m, N) = \frac{2}{N^2}\sum_{T=1}^{N}(N - T)\mathrm{erf}\Big(r/\sqrt{2}\sigma_T\Big)^m \tag{7}$$

where the subscript I refers to the input time series and σ_T^2 is the rate of separation of two inputs with time.

The correlation integral of the *output* x(t) consists of three terms:

$$C_O(r; m, N) = C_{00} + C_{01} + C_{11} \tag{8}$$

C_{00} contains correlations between vectors at the origin; C_{01} contains correlations between pairs of a vector at the origin and a nonzero vector. The last term, similar to (7), contains the correlations between pairs of nonzero vectors. Weighting the three types of correlations by the respective numbers of vector pairs gives C_O.

The weight of each correlation is based on the number of vectors at or off the origin, N_0 and $N_1 = N - N_0$, respectively. The average rate at which vectors are removed from N_0 and added to N_1 is estimated as the autocorrelation function or σ_T

a. m=1.

$$C_{00}(r; 1, N) = \frac{2}{N^2}\sum_{i=1}^{N/2}\sum_{j>i}^{N/2}\Theta(r - |\mathbf{X}_j - \mathbf{X}_i|) = \frac{N_0^2}{N^2} = \frac{1}{4}, \tag{9}$$

$$C_{01}(r; 1, N) = \frac{2}{N^2}\sum_{i=1}^{N/2}\sum_{j=1}^{N/2}\Theta(r - |\mathbf{X}_j - (\mathbf{X}_i = \mathbf{0})|) =$$

$$= \frac{1}{2}\int_0^r P(x)dx = \frac{1}{2}\mathrm{erf}\Big(\mathrm{r}/\sqrt{2}\sigma\Big) \tag{10}$$

and

$$C_{11}(r; 1, N) = \frac{2}{N^2}\sum_{T=1}^{N/2}\left(\frac{N}{2} - T\right)\mathrm{erf}\Big(r/\sqrt{2}\sigma_T\Big). \tag{11}$$

Thus the correlation integral for the output is

$$C_O(r;m=1,N)=\frac{1}{4}+$$
$$+\frac{1}{2}\mathrm{erf}\left(r/\sqrt{2}\sigma\right)+\frac{2}{N^2}\sum_{T=1}^{N/2}\left(\frac{N}{2}-T\right)\mathrm{erf}\left(r/\sqrt{2}\sigma_T\right) \tag{12}$$

b. m>1.

To calculate the vectors that move from N_0 to N_1 as the embedding dimension is increased from m to m+1, one considers the window length, (m-1)τ, versus the autocorrelation. If the window length is large enough so that some of the u(t) in **U** are positive, then the corresponding **X** leaves N_0. The window length is modeled with the diffusion time of the process necessary to reach 0 from u. Thus $\Delta u=u$ and if the process diffuses with characteristic time

$$\sigma_T^2=\left\langle\Delta u^2(T)\right\rangle=\sigma^2R_T^2 \tag{13}$$

where σ is the standard deviation, then the time necessary is $R_T^{-1}(u/\sigma)$. Conversely in time (m-1)τ the points $0<u<\sigma_T$ will have diffused to 0 and the corresponding vectors will move from N_0 to N_1.

Thus the i-th embedding dimension will contribute the following number of points to N_0:

$$\int_{u_i}^{\infty}P(u)du=\frac{1}{\sqrt{\pi}\sigma}\int_{u_i}^{\infty}e^{-(u/\sigma)^2}du=\frac{1}{2}\left(1-erf\left(\frac{u_i}{\sigma}\right)\right) \tag{14}$$

And the number of points in N_0 from all m dimensions is:

$$\frac{N_0}{N}=\left(\frac{1}{2}\right)^m\left(1-erf\left(\frac{u_2}{\sigma}\right)\right)\ldots\left(1-erf\left(\frac{u_{m-1}}{\sigma}\right)\right) \tag{15}$$

The limit of integration u_m is found for two cases:

i) In the case of a Gaussian $1/f^{\alpha}$ noise

$$u_m=\sigma_T=\sigma R[(m-1)\tau] \tag{16}$$

where R(T) is the normalized rate of separation calculated in Theiler (1991). The population of points at the origin becomes

$$\frac{N_0}{N}=\left(\frac{1}{2}\right)^m(1-erf(R(\tau)))\ldots$$
$$\ldots(1-erf(R[(m-2)\tau]))(1-erf(R[(m-1)\tau])) \tag{17}$$

ii) In the case of a Brownian motion diffusing as $\left\langle\Delta u^2(T)\right\rangle^{1/2}\sim T^H$ (Mandelbrot and Van Ness, 1968)

$$u_m=\sigma\left(\frac{T_w-T_{AC}}{T_{AC}}\right)^{H/2}=\sigma(m-1)^{H/2} \tag{18}$$

and thus the population N_0 is:

$$\frac{N_0}{N}=\left(\frac{1}{2}\right)^m(1-erf(1))\ldots$$
$$\ldots\left(1-erf\left((m-2)^{H/2}\right)\right)\left(1-erf\left((m-1)^{H/2}\right)\right) \tag{19}$$

To calculate C_O one needs to weight the three contributions to C_O(m=1) appropriately.

$$C_O(r;m,N)=\left(\frac{N_0}{N}\right)^2+\frac{2N_0N_1}{N^2}\mathrm{erf}\left(r/\sqrt{2}\sigma\right)+$$
$$+\frac{2}{N^2}\sum_{T=1}^{N_1}(N_1-T)\mathrm{erf}\left(r/\sqrt{2}\sigma_T\right) \tag{20}$$

As m increases and N_0, C_{00}, and C_{01} decrease, there will be a transition from a flat profile of C(r) at m=1 to a regular scaling profile of C(r) at m>>1 (Fig. 9). The sharpness of the transition depends on how abruptly R[(m-1)τ] changes with m which is regulated by the spectral index, α. Thus the sharpest transition from low to high embedding dimensions is expected at high $\alpha\sim3$ because for those values R increases most abruptly and $\sigma=\sigma(\alpha)$ is smallest.

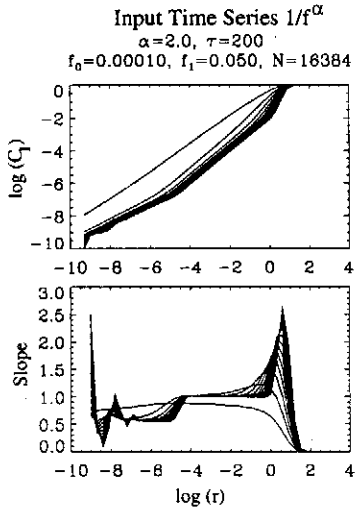

Fig. 9. The correlation integrals and its slope for a $1/f^{\alpha}$-noise input time series (upper panels) and for the output of the rectifier (lower panels). The parameters that determine the input time series are described in (Theiler, 1991). (cont.)

4.5 The effect of a rectifier to the solar wind input in the magnetosphere.

The correlation integrals of vB_z and vB_{South} (Figs. 10, 11) mirror the integrals obtained with the inputs R(t) and L(t) above (Figs. 3, 5, 7, 8). There are two regimes for the correlation integral of vB_{South} depending on m. The locl slope in the lower regime is <1 while for the higher regime it is ~2. The slope for the higher regime agrees with the unrectified vB_z (Fig. 10) and is somewhat lower than the dimension scaling observed for $1/f^{\alpha}$ noise (Osborne and Provenzale, 1989; Theiler, 1991), where α=5/3 for the IMF fluctuation spectrum.

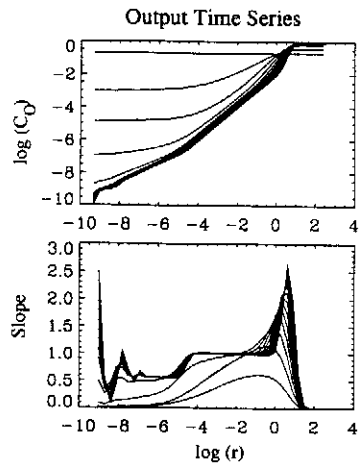

Fig. 9. (Continued) The correlation integrals and its slope for the rectified (output) time series. Note the transition of C_O from a flat correlation integral to the C_I as m is increased.

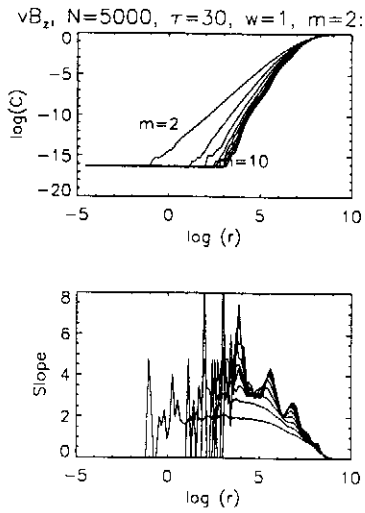

Fig. 10. Correlation diagram and slope of the solar wind convection electric field y-component, vB_z

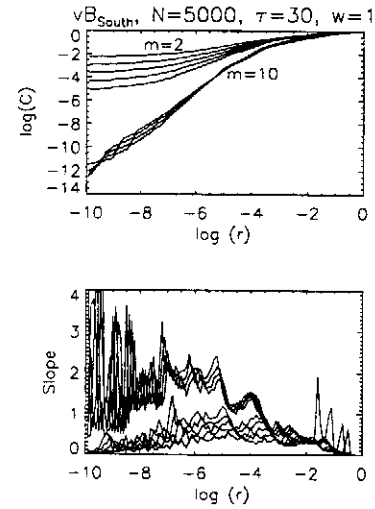

Fig. 11. Correlation diagram and slope of the solar wind rectified electric field vB_{South}.

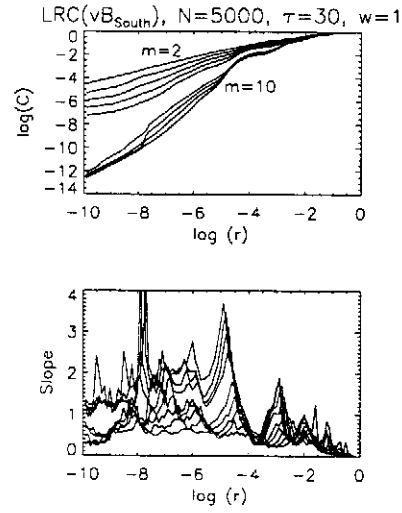

Fig. 12. Passing the rectified input (electric field vB_{South}) through a linear MA filter does not change the correlation diagram and its slope qualitatively.

5 Using the correlation integral to examine a linear model of the solar wind-auroral geomagnetic activity coupling

After the solar wind input has been rectified, it is further processed by the magnetospheric response which is considered as a nonlinear filter (Baker et al., 1990; Goertz et al., 1993; Vassiliadis et al., 1994). One of the outputs is the auroral geomagnetic activity, usually quantified through the auroral electrojet indices AE. In particular, the AL index represents the intensity of the westward auroral electrojet current (Davis and Sugiura, 1966). The auroral electrojets are intensified due to the energy dissipation at the auroral ionosphere during magnetospheric substorms. Therefore AL is essentially a rough estimate of the global dissipation of the energy which is transferred from the solar wind to the Earth magnetosphere and drives the substorms. Further, the AL index is related to nonlinear processes responsible for ionospheric ion extraction and important in the internal magnetospheric dynamics and substorm development (Daglis et al., 1992, 1994). Therefore models of the mapping of solar wind/IMF conditions to the AL index are of great interest to substorm research.

Early models of the solar wind-magnetosphere coupling between vB_{South} and AL were linear "prediction" filters (e.g. Clauer, 1986). These moving averages (MA)

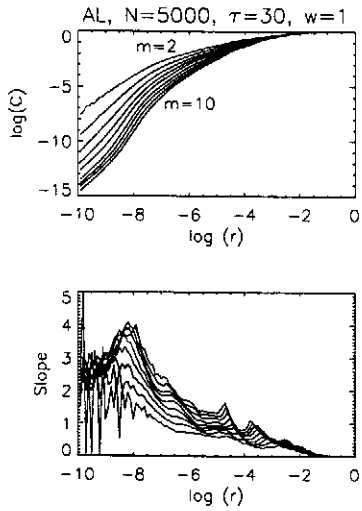

Fig. 13. The observed output AL of the magnetospheric nonlinear filtering of the vB_{South} is qualitatively different than the linear system output (previous Figure).

yield time scales (Bargatze et al., 1985) related to global magnetospheric processes, but reproduce AL observations only qualitatively. A MA filter in the form of an LRC circuit linear model receives the solar wind input and produces an output which is qualitatively similar to the observed AL index (correlation: 60–80%) (Vassiliadis et al., 1993). The correlation integral of the filter-produced AL is very similar to the integral of the rectified input (Fig. 12) showing that the MA filter preserves the transition between two regimes of the rectified vB_{South} (Fig. 11) (note that there is a small increase in the local slope). The preservation of the logC-logr profile is expected for a wide range of parameters of linear moving average filters (Sauer et al., 1991; Broomhead et al., 1992; Abarbanel et al., 1993) although other types of linear filters (autoregressive ones) modify the correlation integral significantly (Badii et al., 1988; Abarbanel et al., 1993).

The correlation integral of the observed AL time series (Fig. 13) is qualitatively different from the LRC circuit output: it has a much narrower scaling range and a higher local slope than the LRC-filtered vB_{South}. The difference in the nonlinear statistic of the two output time series distinguishes the magnetospheric dynamics filter from linear MA filters. It shows that linear MA filters are not appropriate models of the solar wind-auroral geomagnetic activity coupling.

6 Conclusions

A rectifier acting on an input time series is a nonlinear filter which changes the autocorrelation function profile and the probability distribution. The correlation integral was used to quantify these changes by measuring the distribution of pairs of points in the phase space. The change in the correlation integral has been illustrated with two different signals, a random-phase signal and a deterministic signal. The effect of the rectifier was calculated analytically for Gaussian $1/f^{\alpha}$ noise and Brownian motion. For the rectifier the correlation integral of the input time series can be recovered for a high enough embedding dimension m when the window $(m-1)\tau$ is comparable to the length of the average "string of zeros" that the rectifier produces. Depending on the relative size of the two time scales there is a transition between two regimes: the low-slope ("low-dimensional") scaling of the rectified signal at small embeddings and the recovered higher-slope scaling of the original signal at large embeddings. If the window length remains small, the signature of the rectifier in the logC(logr) diagram is a smooth, low local slope (Fig. 8).

The local slope ("dimension") decrease by a simple nonlinear filter such as the rectifier addresses to some extent the claims of Pavlos et al. (1992) for low-dimensionality of the solar wind temperature and IMF |B| after they carefully excluded the possibility of a linearly correlated colored noise. It is interesting how the time series of temperature and IMF |B| appear low-dimensional while related to a turbulent, high-dimensional medium. One answer may be that the temperature and magnetic field are types of nonlinearly correlated noise. Alternatively, considering the effect of the rectifier, the apparent low-dimensional scaling is a consequence of nonlinear filtering of a high-dimensional process, similarly to the decreased slope of the correlation integral of vB_{South}.

The rectifier example shows a method for time series analysis of input-output systems based on applying autonomous techniques to the input and output time series separately. The results should be interpreted as nonlinear statistics of the distribution rather than as descriptions of the stability, complexity, periodicity, etc, as in the autonomous case (note that concepts such as deterministic chaos originally developed for autonomous systems can have analogous meaning for input- output systems if modified appropriately (e.g. Casdagli, 1992)). The use of discriminatory nonlinear statistics was suggested by Theiler et al. (1992a,b) who produced statistical significance tests in their work on detection of nonlinear structure in time series.

Nonlinear statistics can be useful in rejecting or retaining models developed for an input-output system. In the case of the solar wind-magnetosphere coupling the correlation integral was used to discriminate between the output of a linear MA filter and the observed geomagnetic output. The linear MA filter is rejected as model of the coupling since it cannot reproduce the distribution of pairs of points quantified by the correlation integral (although this does not exclude other types of linear models (Price et al., 1993)). Similarly, Klimas et al. (1994) reported using the prediction error as a non-

linear statistic in adjusting some parameters of a nonlinear input-output model to make it similarly predictable to the observed geomagnetic output when driven with the corresponding solar wind input. Additional theoretical research, in particular for multi-input-multi-output systems, is currently under way (D. Prichard and J. Theiler, 1993, private communication). The use of nonlinear statistics to characterize input-output time series is promising in solar wind- magnetosphere coupling and generally in the studies of input-output systems often encountered in geophysics.

Acknowledgments. Discussions with D. A. Roberts are appreciated. D. V. acknowledges an NRC associateship.

References

Abarbanel, H. D. I., R. Brown, and J. J. Sidorowhich, The analysis of observed chaotic data in physical systems, *Rev. Mod. Phys.* 65, no. 4, 1331, 1993.

Badii, R., G. Broggi, B. Derighetti, M. Ravani, S. Ciliberto, A. Politi, and M. A. Rubio, Dimension increase in filtered chaotic signals, *Phys. Rev. Lett.* 60, 979, 1988.

Baker, D. N., A. J. Klimas, R. L. McPherron, and J. Buchner, The evolution from weak to strong geomagnetic activity: an interpretation in terms of deterministic chaos, *Geophys. Res. Lett.* 17, 41-44, 1990.

Bargatze, L. F., D. N. Baker, R. L. McPherron, and E.W. Hones, Magnetospheric impulse response for many levels of geomagnetic activity, *J. Geophys. Res.* 90, 6387-6394, 1985.

Brock, W. A., Nonlinearity and Complex Dynamics in Economics and Finance, in: P. Anderson, K. Arrow, and D. Pines (eds.), *The Economy as an Evolving Complex System.* Addison-Wesley, New York, 1988.

Broomhead, D. S., J. P. Huke, and M. R. Muldoon, Linear filters and non-linear systems, *J. R. Stat. Soc. B* 54, 373, 1992.

Casdagli, M., A dynamical systems approach to modeling input-output systems, in: M. Casdagli and S. Eubank (eds.) *Nonlinear Modeling and Forecasting*, vol. XII of *SFI Studies in the Sciences of Complexity*, p. 265–282. Addison-Wesley, 1992.

Clauer, C. R., R.L. McPherron, C. Searls, Solar wind control of the low-latitude asymmetric magnetic disturbance field, *J. Geophys. Res.* 88, 2123, 1983.

Clauer, C. R., The technique of linear prediction filters applied to studies of solar wind-magnetosphere coupling, 39, Y. Kamide and J. A. Slavin (eds.), *Solar Wind-Magnetosphere Coupling.* Terra Scientific, Tokyo, 1986.

Daglis, I. A., E. T. Sarris, G. Kremser, and B. Wilken, On the solar wind-magnetosphere-ionosphere coupling: AMPTE/CCE particle data and the AE indices, in: *Study of the Solar Terrestrial System*, ESA SP-346, p. 193. ESA/ESTEC, Noordwijk, 1992.

Daglis, I. A., S. Livi, E. T. Sarris, and B. Wilken, Energy density of ionospheric and solar wind origin ions in the magnetotail during substorms, *J. Geophys. Res.* 99, 5691-5703, 1994.

Davis, T. N., and M. Sugiura, The auroral electrojet activity index AE and its universal time variations, *J. Geophys. Res.*, 71, 785, 1966.

Dungey, J. W., Interplanetary magnetic field and the auroral zones, *Phys. Rev. Lett.* 6, 47, 1961.

Grassberger, P., and I. Procaccia, Measuring the strangeness of strange attractors, *Physica D* 9, 189, 1983a.

Grassberger, P., and I. Procaccia, Estimation of the Kolmogorov entropy from a chaotic signal, *Phys. Rev. A* **28**, 2591, 1983b.

Goertz, C. K., R. Smith, and L.-H. Shan, Prediction of geomagnetic activity, *J. Geophys. Res.* 98, 7673, 1993.

Hunter, N. F., Applications of nonlinear time series models to driven systems, in: M. Casdagli and S. Eubank (eds.) *Nonlinear Modeling and Forecasting*, vol. XII of *SFI Studies in the Sciences of Complexity.* Addison-Wesley, 1992.

Hunter, N., and J. Theiler, Characterisation of nonlinear input-output systems using time series analysis, in: S. Vohra, M. Spano, M. Schlesinger, L. Pecora and W. Ditto (eds.), *Proceedings of the First Experimental Chaos Conference.* World Scientific, 1992.

Klimas, A. J., D. N. Baker, D. A. Roberts, D. H. Fairfield, and J. Buchner, A nonlinear dynamical analogue model of geomagnetic activity, *J. Geophys. Res.* 97, 1992.

Klimas, A. J., D. N. Baker, D. Vassiliadis, and D. A. Roberts, Substorm recurrence rates compared during intervals of steady and variable solar wind driving, *J. Geophys. Res.*, submitted, 1994.

Lorenz, E. N., Deterministic nonperiodic flow, *J. Atmos. Sci.* 20, 130, 1963.

Mandelbrot, B., and J. W. Van Ness, *SIAM Rev.* 10, 422, 1968.

McPherron, R. L., Physical Processes Producing Magnetospheric Substorms and Storms, *Geomagnetism* 4, 593–739, 1991.

Osborne, A. R., and A. Provenzale, Finite correlation dimension for stochastic systems with power-law spectra, *Physica D* **35**, 357-381, 1989.

Pavlos, G. P., G. A. Kyriakou, A. G. Rigas, P. I. Liatsis, P. C. Trochoutsos, and A. A. Tsonis, Evidence for strange attractor structures in space plasmas, *Ann. Geophys.* 10, 309, 1992.

Pavlos, G. P., D. Diamandidis, A. Adamopoulos, A. G. Rigas, I. A. Daglis, and E. T. Sarris, Chaos and Magnetospheric Dynamics, Nonlin. Proc. Geophys. 1, in press, 1994.

Prichard, D., and C. P. Price, Spurious dimension estimates from time series of geomagnetic indices, *Geophys. Res. Lett.* 19, 1623, 1992.

Price, C. P., and D. Prichard, The non-linear response of the magnetosphere: 30 October 1978, *Geophys. Res. Lett.* 20, 771, 1993.

Price, C. P., D. Prichard, and J. E. Bischoff, Non-linear input/output analysis of the auroral electrojet index, University of Alaska preprint, 1993.

Roberts, D. A., Is there a strange attractor in the magnetosphere?, *J. Geophys. Res.* 96, 16051, 1991.

Rugh, W. J., *Linear systems theory*, Prentice Hall, Englewood Cliffs, 1993.

Russell, C. T., Solar wind control of magnetospheric configuration, p. 209, in: Y. Kamide and J. A. Slavin (eds.), *Solar Wind-Magnetosphere Coupling.* Terra Scientific, Tokyo, 1986.

Sauer, T., J. A. Yorke, M. Casdagli, Embedology, *J. Stat. Phys* 65, Nos. 3–4, 579, 1991.

Theiler, J., Spurious estimates of correlation dimension, *Phys. Rev. A* 34, 2427, 1986.

Theiler, J., Some comments on the correlation dimension of $1/f^{\alpha}$ noise, *Phys. Lett. A* **155**, 480, 1991.

Theiler, J., S. Eubank, A. Longtin, B. Galdrikian, J. D. Farmer, Testing for nonlinearity in time series: the method of surrogate data, *Physica D* 58, 77, 1992a.

Theiler, J., B. Galdrikian, A. Longtin, S. Eubank, and J. D. Farmer, Detecting nonlinear structure in time series, in: S. Vohra, M. Spano, M. Schlesinger, L. Pecora and W. Ditto (eds.), *Proceedings of the First Experimental Chaos Conference.* World Scientific, 1992b.

Theiler, J., and S. Eubank, Don't bleach chaotic data, Los Alamos preprint LA-UR-92-1575, 1993.

Vassiliadis, D., A. S. Sharma and K. Papadopoulos, Time Series Analysis of Magnetospheric Activity using Nonlinear Dynamical Methods, pp. 341–347, in: T. Bountis (ed.), *Chaotic Dynamics: Theory and Practice.* Plenum, 1992.

Vassiliadis, D., A. S. Sharma, and K. Papadopoulos, An empirical model relating the auroral geomagnetic activity to the interplanetary magnetic field, *Geophys. Res. Lett.* 20, 1731, 1993.

Vassiliadis, D., A. J. Klimas, D. N. Baker, and D. A. Roberts, "A Description of Solar Wind-Magnetosphere Coupling Based on Nonlinear Filters", *J. Geophys. Res.*, submitted, 1994.